Recovery of Copper Nanoparticles from AMD by Cementation with Iron and SDS

G. Granata and C. Tokoro

Abstract In this work, we studied the recovery of copper from AMD by cementation with iron powder. To control the size of copper particles within the nanoscale range, we tested the use of the anionic surfactant sodium dodecyl sulfate (SDS). We tested three concentration levels (0.2, 0.4 and 0.6 M) and temperatures (25, 50 and 75 °C). The activation energy of cementation was also assessed by fitting the experimental data with the Arrhenius equation. Under all investigated conditions, the cementation reaction was found to be a diffusion-controlled process. Without surfactant, the activation energy was 19.9 kJ/mol. In the presence of SDS the activation energy increased up to about 35 kJ/mol. With or without SDS, the particle size of the copper product was strongly affected by the cementation temperature. Without SDS, the cemented product aggregated into micro-sized clusters of about 15 μm at 25 °C, 2–3 μm at 50 °C and 1 μm at 75 °C. The addition of SDS resulted in a dramatic decrease of copper particle size up down to the nanoscale range. Under the best operating conditions, the particle size of copper was <100 nm.

Keywords Copper · Nanoparticles · AMD · Cementation

Introduction

Acid mine drainage (AMD) is the wastewater formed through chemical reaction of ground/surface water with sulfide minerals [1]. Often assisted by bacteria, the reaction results in the formation of sulfuric acid and ferric ion, which in turn promotes the dissolution of other metals from the surrounding rocks [2]. Due to low pH and high concentrations of heavy metals and toxic anions [3], AMD is a severe water pollution problem, especially where sulfide ores are mined. Nevertheless,

G. Granata (✉) · C. Tokoro
Faculty of Science and Engineering, Waseda University,
Okubo 3-4-1, Shinjuku-Ku, Tokyo, Japan
e-mail: giuseppe.granata1307@gmail.com

B. Davis et al. (eds.), *Extraction 2018*, The Minerals, Metals & Materials Series,
https://doi.org/10.1007/978-3-319-95022-8_182

AMD can sometimes represent a potential source of recoverable values such as non-ferrous metals [4] and rare earth elements [5]. This is particularly important for copper, where the promotion of recovery and recycling technologies is desirable since in recent times demand exceeds supply [6]. Therefore, in this work we studied the direct recovery of copper from acid mine drainage by cementation with iron powder.

The cementation between copper and iron can be described through a simplified Eq. (1):

$$Cu^{2+} + Fe^{0} \rightarrow Cu^{0} + Fe^{2+} \quad (1)$$

The reaction has been extensively investigated under different configurations involving the use of iron as powder [7], grid [8], shot [9], spheres [10] and rotating cylinders [11]. Cementation was mostly studied as a solution purification operation in hydrometallurgical processes and no particular attention was paid toward production of high added value products.

Given the recent trends in the production and use of nanomaterials, producing high quality products actually represents an important aspect to be considered. Therefore, we studied a surfactant-assisted cementation to directly produce copper nanoparticles (CuNPs) from the targeted AMD. Due to the increased surface area, CuNPs exhibit enhanced properties compared to their micro-sized counterparts [12]. Higher thermal and electrical conductivity and reduced melting point enables CuNPs to be preferred in many applications, especially in the electronic industry as conductive ink for inkjet printing technology [13].

Aiming to produce CuNPs from a waste stream like AMD, we implemented a factorial design of experiments to investigate the use of sodium dodecyl sulfate (SDS) as a templating agent to control the particle size of copper. We studied the effect of temperature and SDS concentration on cementation kinetics and the particle size distribution of the cemented copper.

Experimental

Materials

The AMD used in this work was generated from the processing of the low grade copper ore at the Erdenet Mine in Mongolia. The experiments were performed from synthetic sulfate solution modeling the real AMD and containing 6 g/L Cu, and 2.6 g/L Fe, 1.1 g/L Mn, 0.05 g/L Zn and 0.05 g/L Cd at pH 3.6. All chemicals used in this study were analytical grade reagents supplied by Wako Pure Chemical Industries (Japan). The iron used for cementation was a 99.9% powder with an average particle size of 45 μm.

Methods

The cementation was carried out upon adjustment of pH from 3.6 to 1.5 to prevent oxidation and precipitation of iron. In each experiment, the as-received iron powder was added to 100 mL of AMD solution at a 1:1 stoichiometric ratio with copper (Cu/Fe = 1). The reaction was conducted for 30 min under stirring and controlled temperature. Sampling was performed at 0.5, 1, 1.5, 2, 3, 5, 10, 20, and 30 min to determine the residual concentration of metals in solution. In the surfactant-assisted cementation, SDS was added and completely dissolved into the initial metals-bearing solution before adding Fe powder. We investigated three levels of SDS concentration (0.2, 0.4, and 0.6 M) and 3 temperature levels (25, 50, and 75 °C). The experiments for studying the kinetics were performed also at 38 °C. Control experiments were performed without surfactants at the same three temperatures.

Analysis and Particle Size Distribution

The concentrations of dissolved metals in the liquid samples were determined by inductively coupled plasma optical emission spectroscopy (ICP-OES, Perkin Elmer, Optima 5300) upon filtration on 45 μm cellulose filters and dilution. The cemented copper was collected by centrifugation (11000 rpm, 5 min), washed with ethanol, dried and stored for analysis. Field-emission scanning electron microscopy (Hitachi S-4500SFE-SEM) was used to determine particle size distribution and morphology. The phase composition of the cemented product was determined using an X-ray diffractometer (Rigaku RINT UtimaIII X-ray diffactometer) with Co Ka radiation (k = 1.789 Å) operated at 40 kV and 20 mA emission.

The size of CuNP was estimated through image analysis of FE-SEM micrographs using Inkscape and ImageJ free software, as elsewhere explained [14].

Results

Cu Recovery and Cementation Kinetics

Experimental results in terms of copper recovery and kinetic parameters are listed in Table 1. With and without surfactant, the highest copper recovery was obtained at 50 °C. The lower recovery observed at 25 °C can be explained as the result of slower kinetics, which prevented quantitative recovery of copper within 30 min. The lower recovery observed at 75 °C could be instead explained by the possible re-oxidation of copper by the Fe^{3+} produced from the oxidation of Fe^{2+} as the experiment was conducted in an air atmosphere.

Table 1 Experimental conditions and results

Surfactant	Temperature (°C)	Max Cu recovery (%)	k ($10^3 \times s^{-1}$)	R^2	Ea (kJ/mol)
None	25	91 ± 13	0.0012	0.9911	19.9
	38	94 ± 10	0.0018	0.9945	
	50	100 ± 1	0.0026	0.9986	
	75	93 ± 6.0	0.0038	0.9991	
SDS 0.2 M	25	90 ± 1	0.0003	0.9596	35.9
	38	91 ± 13	0.0004	0.9977	
	50	94 ± 8	0.0009	0.9707	
	75	95 ± 4	0.0022	0.9925	
SDS 0.4 M	25	83 ± 6	0.00018	0.9866	35.3
	38	88 ± 4	0.00050	0.9953	
	50	99 ± 1	0.00070	0.9924	
	75	87 ± 7	0.00150	0.9903	
SDS 0.6 M	25	86 ± 4	0.00011	0.9917	35.2
	38	92 ± 5	0.00031	0.9845	
	50	97 ± 2	0.00052	0.9981	
	75	89 ± 4	0.00098	0.9991	

The kinetic study of cementation was performed by fitting the experimental data with the Shrinking-core model (SCM). This model was chosen given the heterogeneous nature of the cementation reaction, also resulting in the formation of a solid product, metallic copper, on the iron surface. Furthermore, a previous study used the SCM with ash diffusion to describe the kinetics of copper cementation by iron [15].

According to the model, the common test for diffusion-controlled reactions involves plotting the reacted fraction of copper (x) as $1 - \frac{2}{3}x - (1-x)^{2/3}$ against time. Results of fitting the data are shown in Fig. 1 while the fitting parameters are listed in Table 1. The good straight line fits in Fig. 1 confirmed that the cementation reaction was a diffusion-controlled process. It is reasonable that the diffusion of ions through the metal copper product formed on the iron surface was the step limiting the overall kinetics. The apparent rate constants were found to be the highest for the cementation without surfactant (Fig. 1a; Table 1). The addition of SDS produced a significant decrease in the rate constants, irrespective of the SDS concentration. Increasing the SDS concentration from 0.2 to 0.4 M (Figs. 1b and c) resulted in a six to seven-fold increase in the rate constants. However, the rate constants decreased when the SDS concentration was further increased to 0.6 M (Fig. 1d). Given the physical nature of the controlling mechanism, a possible explanation for these observations could be the increased viscosity of the reaction media when the SDS concentration was the highest. Further experiments will provide more details about this aspect.

Based on the experimental results at different temperatures, the activation energy of cementation with and without SDS was determined. The Arrhenius plots are

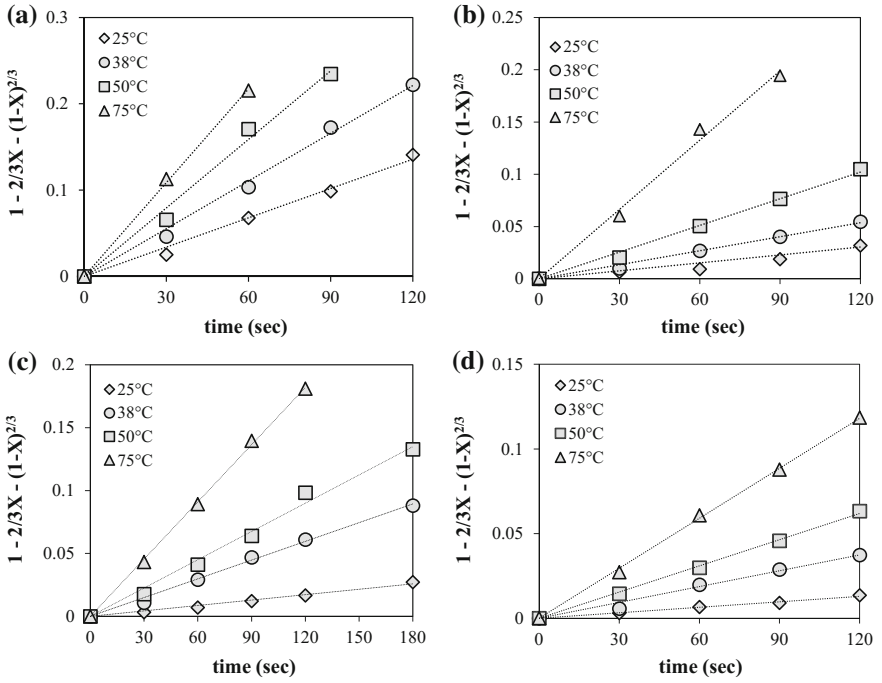

Fig. 1 Fitting of experimental results with SCM-ash diffusion for cementation without surfactant (**a**) and with 0.2 M SDS (**b**), 0.4 M SDS (**c**) and 0.6 M SDS (**d**)

shown in Fig. 2. Without SDS, the activation energy was found to be 19.9 kJ/mol. This value is in substantial agreement with previous studies [11, 16] and with diffusion-controlled reactions. The addition of SDS resulted in a dramatic increase of activation energy up to about 35 kJ/mol under all investigated concentrations. A similar value of activation energy (30 kJ/mol) was also described in previous work as an expression of a diffusion-controlled reaction [15]. However, the increased activation energy observed with SDS suggests a partial shift of controlling mechanism towards a partially chemical or mixed reaction rate control. The increased energy barrier of cementation in the presence of SDS could be reasonably considered as the reason for slower kinetics. In previous works where surfactants were used to modify the interface properties, the addition of SDS also resulted in the increase of activation energy [11]. However, in this work SDS was used as templating agent at significantly higher concentrations. The SDS concentration was not only higher than the critical micellar concentration (CMC) but also at least double that of Cu^{2+}. Under these conditions, SDS in aqueous media can self-assemble into spherical or rodlike micelles that can promote metal reduction around the spatially confined hydrophilic volume [17]. In addition, SDS molecules can coordinate the cupric ion with two dodecyl sulfate groups [14]. As a consequence, the alkyl chains surrounding the metal ion would hinder the diffusion of

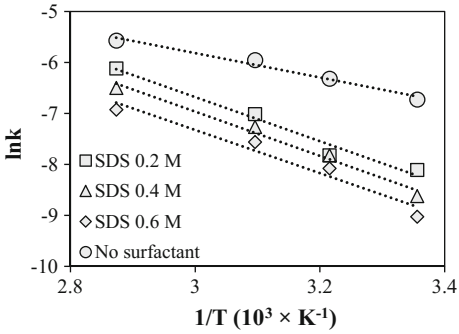

Fig. 2 Activation energy of cementation with and without SDS

more cupric ion and/or iron by steric effect, thereby retarding the kinetics [18]. This phenomenon inhibits the kinetics but it is also responsible for limiting the aggregation and/or crystal growth of metal particles.

Characterization of Cemented Copper

The results of the characterization of the cemented copper are given in Table 2. Under all investigated conditions, the cemented product was found to be face-centered cubic (FCC) copper crystals (XRD spectra not shown here). However, the XRD spectra of products obtained at 25 °C also exhibited the peaks of α-iron. The presence of residual iron in the solid product after 30 min cementation at low temperature was the consequence of incomplete reaction due to slower kinetics. Accordingly, the copper grade of products cemented at 25 °C, determined

Table 2 Characteristics of cemented copper

Surfactant	Temperature (°C)	P60 diameter (nm)	Phase composition	Cu grade (%)
None	25	16400 ± 604	Cu	97.08
	50	3338 ± 317	Cu	98.47
	75	1247 ± 417	Cu	98.75
SDS 0.2 M	25	547 ± 252	Cu, Fe	96.65
	50	246 ± 72	Cu	99.15
	75	100 ± 27	Cu	99.34
SDS 0.4 M	25	254 ± 82	Cu, Fe	97.85
	50	152 ± 69	Cu	98.98
	75	94 ± 8	Cu	99.03
SDS 0.6 M	25	351 ± 94	Cu, Fe	97.18
	50	192 ± 76	Cu	99.05
	75	132 ± 58	Cu	99.22

by dissolution and ICP analysis, was about 97%. In contrast, the copper grade was the highest at 50 and 75 °C, at about 99% depending on the specific operating conditions (Table 2). Although the Cu grade was about 98–99%, the concentrations of Fe, Mn, Zn and Cd in the cemented copper were below the detection limit of our ICP-OES. This evidence suggests that the surface of CuNPs might have oxidized slightly.

The FE-SEM micrographs of the copper cemented without surfactant are shown in Fig. 3 while the particle size distribution curves determined from the micrographs in Fig. 3 are shown in Fig. 4. The average P60 diameter of copper particles without surfactant ranged from a maximum of 16 μm at 25 °C to a minimum of about 1.2 μm at 75 °C. Temperature exhibited a key role in determining the particle size of cemented copper. This evidence could be reasonably explained in terms of kinetics. A faster reaction determines the production of a larger number of copper nuclei within the same time range. Therefore, each nucleus will grow to a lesser extent and the resulting particles will be smaller. In spite of this evident decrease of particle size, the copper particles aggregated into micro-clusters upon crystallization.

Using SDS at the tested dosages of 0.2, 0.4 and 0.6 M appeared to prevent particles from growing and/or aggregating. The FE-SEM micrographs of the copper product cemented in the presence of SDS are shown in Fig. 5. The particle size distribution curves determined from the micrographs in Fig. 5 are shown in Fig. 6. The addition of SDS produced a dramatic decrease of particle size down to the nanoscale range. Particle size control was achieved because of the ability of SDS to coordinate the cupric ion in solution with its anionic head. In this way, the SDS

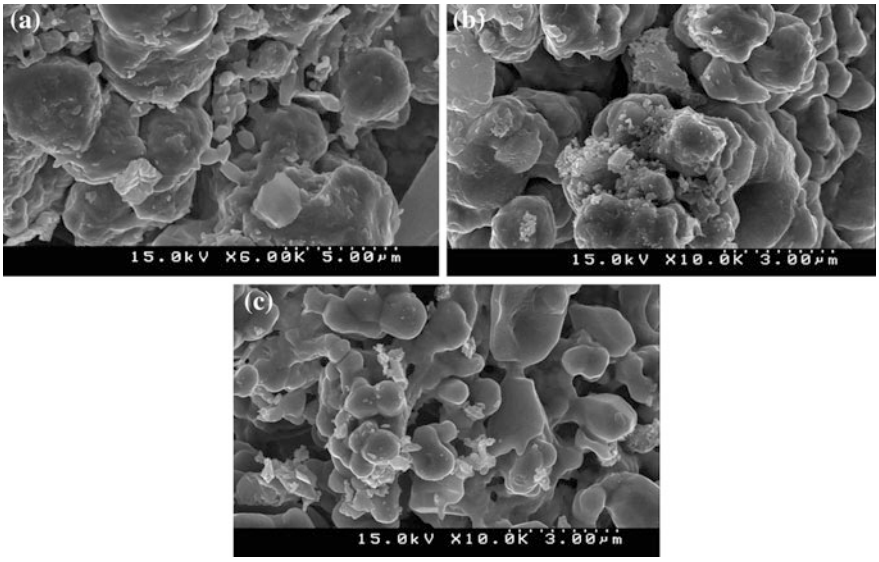

Fig. 3 FE-SEM micrographs of copper cemented without surfactant at **a** 25 °C, **b** 50 °C, **c** 75 °C

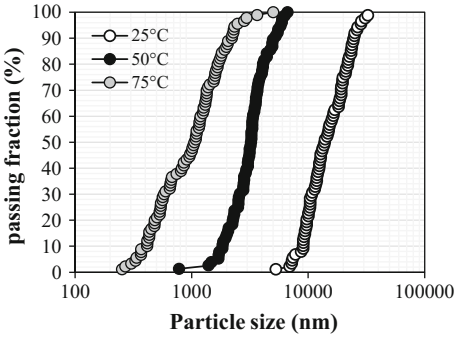

Fig. 4 Particle size distribution of copper cemented without SDS

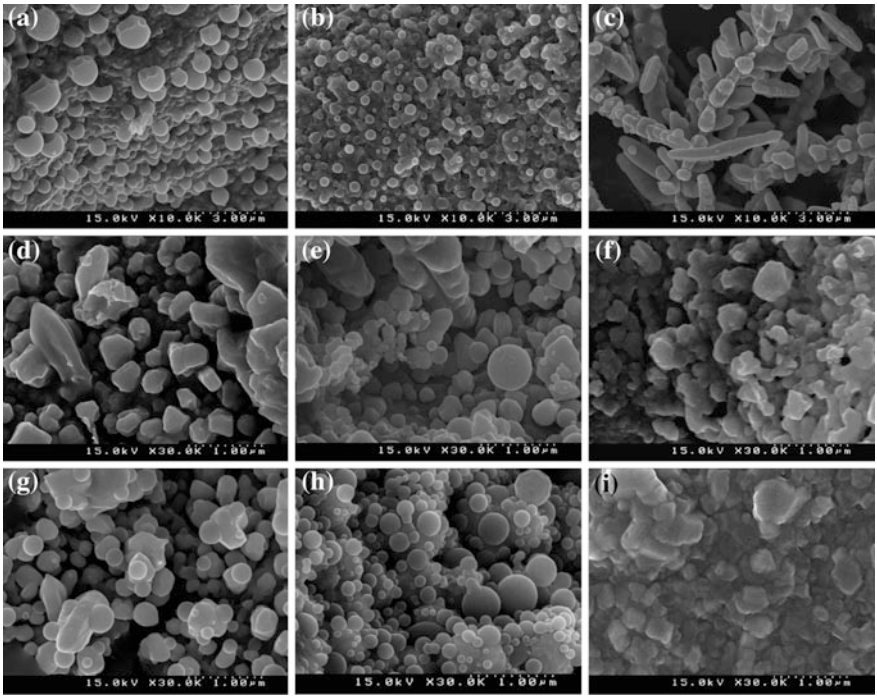

Fig. 5 FE-SEM micrographs of copper cemented with: 0.2 M SDS at **a** 25 °C, **b** 50 °C, **c** 75 °C, with 0.4 M SDS at **d** 25 °C, **e** 50 °C, **f** 75 °C with 0.6 M SDS at **g** 25 °C, **h** 50 °C, **i** 75 °C

alkyl chains surrounding the as-formed copper nuclei can hinder crystal growth and/or aggregation by a steric effect. Regardless of the SDS concentration, temperature played once more a key role in affecting the copper particle size. The average P60 diameter was generally highest at 25 °C and lowest at 75 °C.

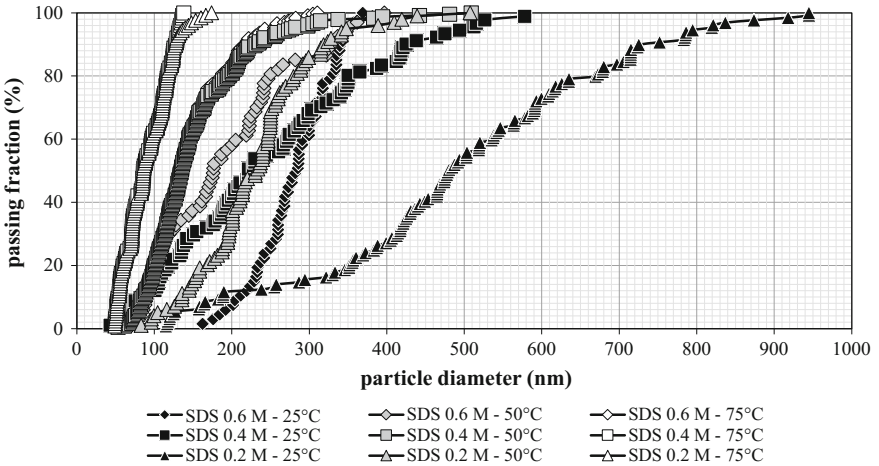

Fig. 6 Particle size distribution of copper cemented with SDS

The general effect associated with the increase of SDS concentration from 0.2 to 0.4 M, was a slight decrease of the P60 diameter, especially from low temperature. In contrast, a further increase of SDS concentration up to 0.6 M did not cause any significant decrease in particle size. Although temperature played an important role in controlling the copper particle size, the use of SDS was crucial to keep the size within the nanoscale range. Interestingly, the copper particles obtained at 75 °C in the presence of 0.4 M SDS exhibited an average P60 diameter lower than 100 nm.

As for morphology, whereas spherical nanoparticles were obtained with 0.2 and 0.4 M SDS, irregular spheres and elongated aggregates were obtained with 0.6 M SDS. The increased anisotropic growth might be a consequence of an excess of dodecyl sulfate coordinating not only Cu^{2+} but also the co-existing ions. In turn, the presence of other ions within the surfactant aggregates and during the formation of nanoparticles might have reduced the isotropy.

Conclusions

Copper was successfully recovered from AMD by cementation with iron. The cementation kinetics was found to be a diffusion-controlled process with an activation energy of 19.9 kJ/mol. Temperature played a key role in regulating reaction kinetics and copper particle size. By adding the surfactant SDS, the particle size of copper decreased down to the nanoscale range. Under the best operating conditions, 99% of the copper could be recovered from the simulated AMD feed solution as nanoparticles with P60 of 95 nm and purity greater than 99%.

References

1. Johnson DB, Hallberg KB (2005) Acid mine drainage remediation options: a review. Sci Total Environ 338(1–2)Special Issue:3–14
2. Kefeni KK, Msagati TAM, Mamba BB (2017) Acid mine drainage: prevention, treatment options, and resource recovery: a review. J Clean Prod 151:475–493
3. Sheoran AS, Sheoran V (2006) Heavy metal removal mechanism of acid mine drainage in wetlands: a critical review. Miner Eng 19(2):105–116
4. Wang LP et al (2014) Selective precipitation of copper and zinc over iron from acid mine drainage by neutralization and sulfidization for recovery. Int J Soc Mater Eng Resour 20(2): 136–140
5. Ayora C et al (2016) Recovery of rare earth elements and yttrium from passive-remediation systems of acid mine drainage. Environ Sci Technol 50(15):8255–8262
6. Watling HR (2014) Chalcopyrite hydrometallurgy at atmospheric pressure: 2. Review of acidic chloride process options. Hydrometallurgy 146:96–110
7. Ku Y, Chen CH (1992) Kinetic study of copper deposition on iron by cementation reaction. Sep Sci Technol 27(10):1259–1275
8. Yahiaoui I, Aissani-Benissad F (2010) Experimental design for copper cementation process in fixed bed reactor using two-level factorial design. Arab J Chem 3(3):187–190
9. Gros F, Baup S, Aurousseau M (2008) Intensified recovery of copper in solution: cementation onto iron in fixed or fluidized bed under electromagnetic field. Chem Eng Process Process Intensif 47(3):295–302
10. Dib A, Makhloufi L (2004) Cementation treatment of copper in wastewater: mass transfer in a fixed bed of iron spheres. Chem Eng Process Process Intensif 43(10):1265–1273
11. El-Batouti M (2005) Removal of copper metal by cementation using a rotating iron cylinder. J Colloid Interface Sci 283(1):123–129
12. Mittu R (2016) Synthesis, characterization of copper nanoparticles-a review. Int Adv Res J Sci Eng Technol 3(5):37–40
13. Calvert P (2010) Inkjet printing for materials and devices. Chem Mater 13(10):3299–3305
14. Granata G, Yamaoka T, Pagnanelli F, Fuwa A (2016) Study of the synthesis of copper nanoparticles: the role of capping and kinetic towards control of particle size and stability. J Nanoparticle Res 18(5):133–145
15. Pal P et al (2017) Copper deposition and formation of nano-particles copper deposition and formation of nano-particles. Sep Sci Technol 49(17):2728–2733
16. Demirkiran N, Ekmekyapar A, Künkül A, Baysar A (2007) A kinetic study of copper cementation with zinc in aqueous solutions. Int J Miner Process 82(2):80–85
17. Tao AR, Habas S, Yang P (2008) Shape control of colloidal metal nanocrystals. Small 4(3): 310–325
18. Cushing BL, Kolesnichenko VL, O'Connor CJ (2004) Recent advances in the liquid-phase syntheses of inorganic nanoparticles. Chem Rev 104(9):3893–3946